Research in Veterinary Science 140 (2021) 6–17

Contents lists available at ScienceDirect

Research in Veterinary Science

journal homepage: www.elsevier.com/locate/rvsc

Computed tomography is superior to radiography for detection of feline elbow osteoarthritis

Charles J. Ley [a,*], Alexandra Leijon [b], Margareta Uhlhorn [c], Leticia Marcelino [c], Kerstin Hansson [a], Cecilia Ley [b]

[a] Department of Clinical Sciences, Swedish University of Agricultural Sciences, SE-750 07 Uppsala, Sweden.
[b] Department of Biomedical Sciences and Veterinary Public Health, Swedish University of Agricultural Sciences, SE-750 07 Uppsala, Sweden
[c] University Animal Hospital, Swedish University of Agricultural Sciences, SE-750 07 Uppsala, Sweden

ARTICLE INFO

Keywords:
Anconeal
Cartilage
Cat
Joint
OA
Osteophyte

ABSTRACT

Elbow osteoarthritis (OA) is common in cats and radiography is typically used for diagnosis. However computed tomography (CT), with its multiplanar three-dimensional characteristics, could have significant advantages for assessment of OA compared to radiography, particularly early in the disease process. The study objectives were to compare radiography and CT to histologic OA changes, investigate the stage of OA that radiography and CT detect, and search for specific changes in CT images strongly predictive for feline elbow OA.

Right elbows from 29 cats were evaluated by radiography and CT, and articular cartilage lesions graded histologically and macroscopically. Three further joints were sampled to specifically evaluate the morphology of the anconeal process. Macroscopic, radiographic and CT OA diagnosis were compared to the reference standard histologic OA that was divided into mild, moderate and severe. Osteophytic spurs on the lateral margin of the anconeal process could be reliably measured in CT images (intra-class correlation 0.79) and when ≥0.5 mm had high sensitivity for moderate/severe histologic OA, moderate sensitivity for mild histologic OA and high specificity for all stages of OA. In moderate/severe histologic OA both radiography and CT subjective OA diagnosis had moderate to very high sensitivity. However, in mild histologic OA CT grading had low sensitivity and radiography did not detect OA. In conclusion, CT of the feline elbow including measurement of osteophytes on the anconeal process lateral margin is superior to radiography for OA detection and should be considered for OA diagnosis, particularly when mild OA changes are of interest.

1. Introduction

Understanding the potential and limitations of diagnostic imaging methods for osteoarthritis (OA) detection is important both for the identification of clinical disease and in research settings where determination of OA status is desired. Osteoarthritis is common in cats, and radiography is currently the most common method for OA diagnosis (Clarke and Bennett, 2006; Clarke et al., 2005; Freire et al., 2011; Godfrey and Vaughan, 2018; Godfrey, 2005; Hardie et al., 2002; Lascelles et al., 2010; Slingerland et al., 2011). Radiographic signs of OA are reported to be present in up to 91% in of cats in an age balanced study (Lascelles et al., 2010), and the elbow is one of the most commonly and severely affected joints (Clarke and Bennett, 2006; Freire et al., 2011; Godfrey and Vaughan, 2018; Godfrey, 2005; Hardie et al., 2002; Lascelles et al., 2010; Slingerland et al., 2011). Radiological OA lesions in the feline elbow have however only been correlated with macroscopic OA diagnosis and only investigated in regard to radiography (Freire et al., 2011). Thus, little is known about diagnostic imaging features of feline OA during the period when the first structural changes of OA occur, and this information is important for studies of OA risk factors, OA biomarkers and investigations of possible disease-modifying OA drugs (Palmer et al., 2013).

Radiographs provide two-dimensional information, which means that changes in the image that are not on, or not close to the edge of skeletal structures are summated on other skeletal structures and may not be visible. This is a significant limitation for using radiographs for OA diagnosis (Guermazi et al., 2008; Turmezei and Poole, 2011). A study in cats comparing radiographic evaluation to macroscopic articular cartilage appearance concluded that radiographic findings do not relate well to cartilage degeneration and other modalities should be

* Corresponding author.
E-mail addresses: charles.ley@slu.se (C.J. Ley), cecilia.ley@slu.se (C. Ley).

https://doi.org/10.1016/j.rvsc.2021.07.025
Received 26 March 2021; Received in revised form 10 June 2021; Accepted 22 July 2021
Available online 24 July 2021

investigated (Freire et al., 2011). The multiplanar three-dimensional (3D) characteristics of computed tomography (CT) imaging means that this technique is likely to have significant advantages over radiography for assessment of individual joints for OA, particularly in the assessment of mild skeletal changes (Turmezei and Poole, 2011), and this may allow for the diagnosis of OA at an earlier stage than radiography. Additionally, whole-body CT scans of animals the size of cats are possible and this provides information from all joints in the body, allowing for vastly improved diagnostic possibilities in regard to overall joint status. It is generally accepted that radiographs detect only severe/advanced OA (Guermazi et al., 2008; Jones et al., 2004; Palmer et al., 2013), but the stage of feline OA that is detected by CT is not clear and studies that investigate whether CT is superior to radiography for OA diagnosis in cats are lacking.

The objective of this study was to compare the sensitivity and specificity of radiography and CT to a reference standard (joint histology) for the diagnosis of OA, and, based on severity of cartilage lesions, to determine what histologic grade of OA these imaging modalities detect. A further objective was to search for specific changes in CT images that were strongly predictive for OA. Based upon the presumption that CT is superior for the diagnosis of feline elbow OA compared to radiography, our hypothesis was that CT would detect OA at a milder/earlier stage than radiography.

2. Materials and methods

2.1. Study population

This study was performed post-mortem, on cats submitted to the Section of Pathology at the Swedish University of Agricultural Sciences in Uppsala, Sweden for necropsy and/or specifically donated by the owner for participation in research. Owner consent for using the animal in research was given for all cats. Cats over 12 months of age, presented for reasons other than elbow disease and without a clinical suspicion of immune-mediated joint disease, were included. Due to its chondrodysplastic predisposition, no individual of the Scottish Fold breed was included (Malik et al., 1999). All but one cat were examined by imaging and macroscopy either the same day or the day after euthanasia. One animal was examined two days after euthanasia. Twenty-nine cats were initially examined and included for elbow grading. Following completion of grading, 3 cats previously collected in another study where whole-body CT images and formalin fixed tissues of elbows were available were sampled to specifically evaluate the morphology of the anconeal process by light microscopy.

2.2. Diagnostic imaging

Radiographs were taken of the right elbow using a computed radiography system (Fujifilm FCR XG-1, Tokyo, Japan) and x-ray system (Adora RF CPI, Nordisk Röntgen Teknik A/S, Hasselager, Denmark) with focal spot film distance 90 cm, exposure settings 50 kVp and 2.5–5 mAs (dependant on tissue thickness). Mediolateral in neutral position and craniocaudal projections were taken.

The CT images were obtained using a third generation, 64 slice multidetector CT scanner (Definition, Siemens Medical Systems, Erlangen, Germany). Transverse images were acquired using: 250 kV, 160 mAs, slice thickness 0.6 mm, slice increment 0.3 mm, focal spot 1.2 mm, high-resolution kernel (B70s) and field of view 156–249 mm. Cats were positioned on a conforming foam cushion in ventral recumbency, without further positioning devices, with the front legs extended cranially, the hind legs extended caudally and the head towards the gantry.

2.3. Evaluation of radiographs and CT images

All radiographs and CT images were assessed in DICOM format by three evaluators (CJL, KH, MU for image grading and CJL, KH, LM for anconeal spur measurement) with image viewing software (Horos, www.horosproject.org). All images were coded, identification information hidden and the order of the presentation of the cats randomised. Individual grading of the radiographs was completed before grading of CT images. A preliminary grading of radiographs and CT images had been done by one evaluator (CJL) more than 2 ½ years before, the other evaluators had not seen the images prior to the grading/measurement done in this study and did not see the CT images until individual grading of the radiographs was completed. The evaluators of the image grading were specialist veterinary radiologists, each with more than 14 years' experience since board certification. Prior to the grading the evaluators met three times for one-hour long meetings, where selected feline OA literature (Freire et al., 2014; Freire et al., 2011) was discussed.

Table 2
Criteria for radiography/computed tomography osteoarthritis (OA) diagnosis in feline elbow joints.

Presence of OA
At least one grade 2, 3 or 4 marginal osteophyte or At least one grade 1 marginal osteophyte and at least 1 of the following: • increased joint soft tissue volume • a discrete area of articular mineral attenuation/opacity in regions other than the expected location of the supinator sesamoid • ≥ grade 1 for central osteophyte • ≥ grade 1 for enthesophyte • ≥ grade 1 for sclerosis • ≥ grade 1 for lysis

Table 1
Computed tomography and radiography subjective lesion grades used for osteoarthritis diagnosis in feline elbow joints.

Lesion category	Grade				
	0	1	2	3	4
Marginal osteophyte/s	No	Suspected	Small	Moderate	Large
Central osteophyte/s	No	Suspected	Small	Moderate	Large
Enthesophyte/s	No	Suspected	Small	Moderate	Large
Subchondral bone sclerosis region/s	No	Suspected	Mild	Moderate	Severe
Subchondral bone lysis region/s	No	Suspected	Mild	Moderate	Severe
Mineral attenuation/opacity[a]	No	Present, divided by maximum cross-sectional area into small (≤ 2.25 mm^2) and large (> 2.25 mm^2)			
Mineralised supinator sesamoid	No	Present, divided by maximum cross-sectional area into small (≤ 2.25 mm^2) and large (> 2.25 mm^2)			
Joint soft tissue volume	Normal	Increased, no other grades			

[a] Discrete areas of articular mineral attenuation/opacity within or adjacent to the joint and not considered to be a mineralised supinator sesamoid.

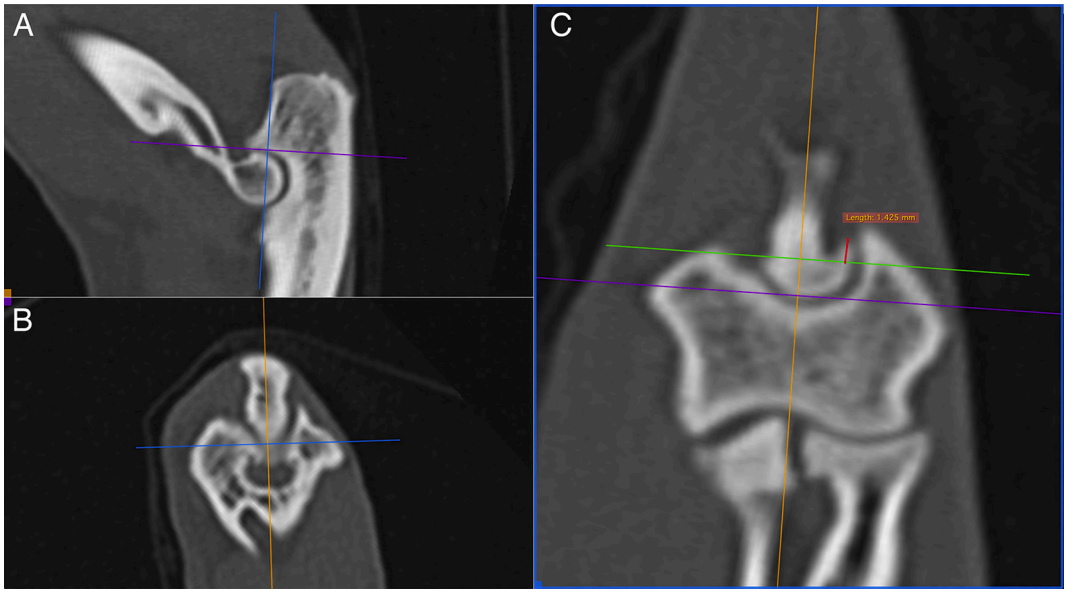

Fig. 1. Multiplanar reconstruction computed tomography images in sagittal (A), transverse (B) and frontal (C) planes of the right elbow joint from an 8-year-old neutered male Domestic Shorthair cat showing the orientation of image planes and measurement method for an anconeal process spur. Measurements were done in the frontal plane. The base of the spur was determined by drawing a 'base line' (green line) line parallel to the transverse plane (purple line) and moving this to align it with the most distal aspect of the medial margin of the spur. A measurement line (red line) was made from, and approximately perpendicular to, the 'base line' to the proximal tip of the anconeal spur. (For interpretation of the references to colour in this figure legend, the reader is referred to the web version of this article.)

Table 3
Classification of overall severity of histologic changes in feline elbow joints.

Severity	Criteria[a]
Normal	GCS $\leq$ 5, no lesion >1
Minimal cartilage change	GCS $\leq$ 7.5, worst lesion 1.5–2.5
Mild osteoarthritis	GCS $\leq$ 7.5, focal lesion $\geq$3; or GCS 8–12.5
Moderate osteoarthritis	GCS 13–22.5
Severe osteoarthritis	GCS 23–32.5

[a] Based upon the global cartilage score (GCS) and the individual lesion grades in each of the five assessed cartilage regions for the elbow joint.

Additionally, evaluators tested the grading of CT images and radiographs using images from another study cohort and discussed these gradings during the meetings. All tools in the imaging software including were available for use by the evaluators and CT images were examined using 3D multiplanar reconstruction (MPR) using imaging planes created independently by the evaluators. Final grades were determined by majority consensus with evaluators first grading the images independently and then meeting for a consensus discussion to reach agreement on grades where there was not majority consensus.

The following lesion categories were subjectively graded either for both presence and severity or for presence only: marginal osteophyte (focal bone formation on the joint margin not considered an

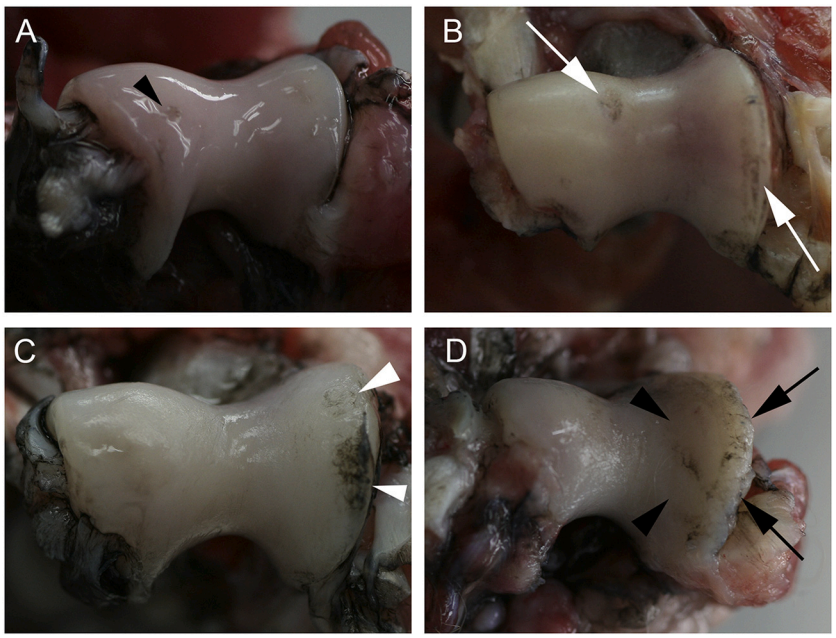

Fig. 2. Representative examples of macroscopic articular cartilage lesion grades on the articular surface of the distal humerus, shown after application and blotting of India ink. (A) Minimal grade lesion showing a small area of surface irregularity/fibrillation with subtle India ink uptake (black arrowhead). (B) Mild grade lesion showing small partial thickness erosions (white arrows). (C) Moderate grade lesion showing a large partial thickness erosion (white arrowheads). (D) Severe grade lesion showing full thickness erosions (black arrowheads), joint surface remodeling and marginal osteophyte formation (black arrows).

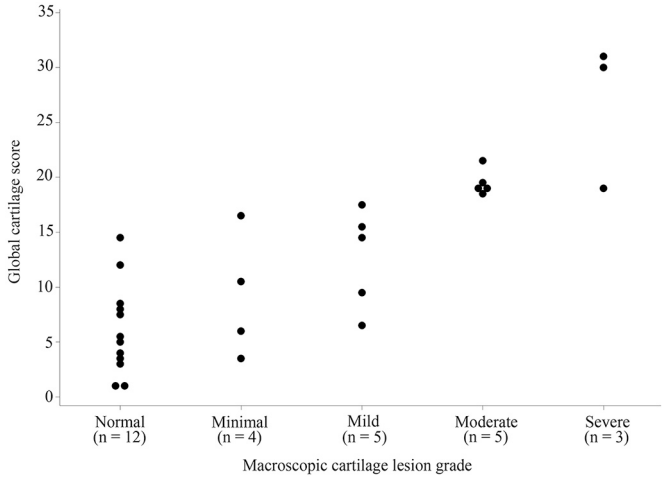

Fig. 3. Distribution of macroscopic cartilage changes according to the histologic global cartilage score in feline elbow joints ($n = 29$).

enthesophyte), central osteophyte (focal bone formation on the articular surface), enthesophyte (focal bone formation in regions of expected soft tissue attachments), subchondral bone sclerosis (increased subchondral bone attenuation/opacity/thickness), subchondral bone lysis (decreased attenuation/opacity of the subchondral bone, including defects on the articular surface and cyst-like lesions), discrete mineral attenuation/opacity, and increased joint soft tissue volume (Table 1). Sclerosis or lysis that was localized to the trabecular bone of the humerus/radius/ulna only and did not extend into or involve the compact subchondral bone was not considered to be subchondral sclerosis/lysis. Due to uncertainty of the intra- or extra-articular location of discrete mineral attenuation/opacity it was decided in the final consensus grading to include these in one group (discrete articular mineral attenuation/opacity). If discrete mineral attenuation/opacity was detected in the reported location of the supinator sesamoid (Wood et al., 1995), these were classified separately as mineralised supinator sesamoids. After grading, one evaluator (CJL) used the freehand region of interest tool in CT images to measure the maximum cross-sectional area of the largest discrete mineral attenuation in the reported location (Wood et al., 1995) of mineralised supinator sesamoid and the largest discrete mineral attenuation not in the location of the supinator sesamoid. Cross-sectional areas of discrete mineral attenuations were considered to be small when $\leq$2.25 mm^2 and moderate to large when >2.25 mm^2 (Voss et al., 2017). In CT images mineral attenuation was considered to be >350 Hounsfield units.

Joints were then classified as radiographic OA-positive (Rad OA) and CT OA-positive (CT OA) depending on radiographic and CT findings respectively, using the grading criteria in Table 2.

To investigate the diagnostic significance of spur-shaped conformations on the lateral margin of the anconeal process, spurs were measured in CT images orientated in standard planes (Fig. 1). Three-dimensional MPR images were orientated with the sagittal plane parallel to the long axis of the olecranon and the transverse plane parallel to the short axis of the olecranon. The image axes were then moved so that the sagittal plane image was located at the level of the axial aspect of the lateral coronoid process and the frontal plane at the level of the radioulnar articulation. The frontal plane was orientated to pass along the most dorsoproximal surface of the olecranon and the cranial aspect of the lateral coronoid process. In the resulting frontal plane image series the maximum proximal to distal dimension of the largest anconeal spur was measured in mm. The base of the spur was determined by drawing a 'base line' parallel to the transverse plane and moving this to align it with the most distal aspect of the medial margin of the spur and a measurement line was made from, and approximately perpendicular to, the 'base line' to the proximal tip of the anconeal spur (Fig. 1).

Fig. 4. Representative examples of radiography lesion grades. Mediolateral (A) and craniocaudal (B) projections from a 23-year-old cat showing a suspected (grade 1) osteophyte (arrow). Mediolateral (C) and mildly oblique craniocaudal (D) projection a 5-year-old cat showing small (grade 2) osteophytes (arrows) and a large mineral opacity in the expected region of the supinator sesamoid (black arrow). Mediolateral (E) and craniocaudal (F) projections from a 12-year-old cat showing moderate (grade 3) osteophytes (arrows) and two small discrete mineral opacities (black arrows). Mediolateral (G) and craniocaudal (H) projections from a 19-year-old cat showing large (grade 4) osteophytes (arrows), multiple discrete mineral opacities (black arrows) and multiple areas of severe sclerosis (white arrowheads) and lysis (black arrowheads).

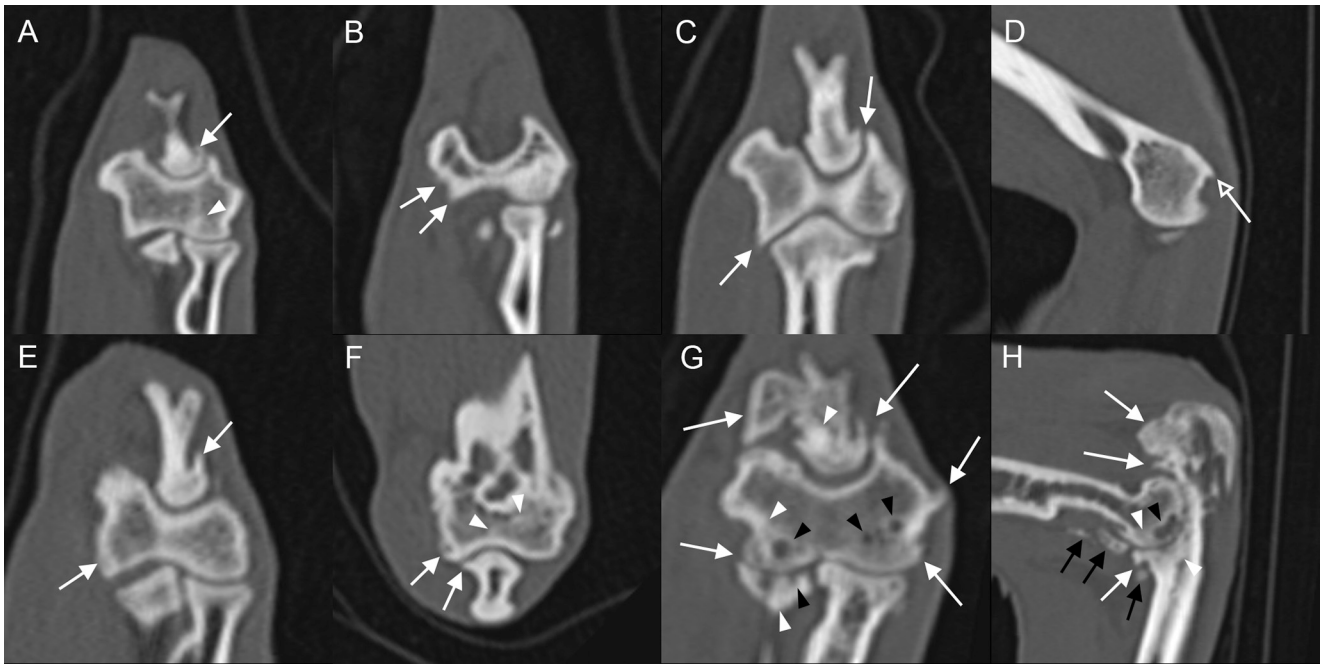

Fig. 5. Representative examples of computed tomography lesion grades. Frontal plane images (A and B) from a 12-year-old cat showing suspected (grade 1) osteophytes (white arrows) and suspected sclerosis (white arrowhead). Frontal (C) and sagittal (D) plane images from a 5-year-old cat showing small (grade 2) osteophytes (white arrows) and a moderate (grade 3) enthesophyte (open arrow). Frontal plane images (E and F) from a 5-year-old cat showing moderate (grade 3) osteophytes (white arrows) and mild (grade 2) sclerosis (white arrowheads). Frontal (G) and sagittal (H) images from a 19-year-old cat showing large (grade 4) osteophytes (white arrows), moderate (grade 3) sclerosis (white arrowheads), severe (grade 4) lysis (black arrowheads) and multiple discrete mineral attenuations (black arrows).

2.4. Macroscopic assessment of articular cartilage

Following diagnostic imaging, the right elbow joint was opened by incision of the joint capsule. In the cohort of 29 cats the articular cartilage was painted with India ink (Lefranc & Bourgeois, Le Mans Cedex, France) diluted 1:5 in 0.9% sodium chloride solution to more accurately visualize cartilage defects. The ink was then removed by gently blotting the cartilage surface with gauze moistened with 0.9% sodium chloride solution. Presence of OA was based on articular cartilage lesion severity and were subjectively graded by one evaluator (CL) as: grade 0) normal = no cartilage lesions, grade 1) minimal = dull and/or discoloured cartilage and/or minimal surface irregularity/fibrillation, grade 2) mild = distinct surface irregularity/fibrillation and/or small partial thickness erosion, grade 3) moderate = large partial thickness erosion and/or small full thickness erosion, and grade 4) severe = large erosion with/without change in joint surface contour. For statistical analysis grade 0 and 1 were considered macroscopic OA-negative and grades 2, 3 and 4 macroscopic OA-positive (Macro OA).

The additional three joints specifically used for histologic evaluation of the anconeal process were all left elbow joints. These were not graded as part of this study, and had no India ink applied to the joint surfaces.

2.5. Sampling for histology

Joints (n = 32) were fixed in 10% neutral buffered formalin and decalcified in formic acid (20% *v*/v, Kristensens lösning, Solveco AB, Rosersberg, Sweden). Following decalcification, osteochondral tissues including the full thickness of the articular cartilage and adjacent subchondral bone, were obtained for histologic examination. Samples for histologic cartilage lesion grading (n = 29 joints) were obtained from the humeral condyle in a frontal plane (including the trochlea and capitulum), from the ulna in a parasagittal plane, including the anconeal and coronoid processes, and from the radius in a frontal or an oblique frontal plane. Sampling was guided by the macroscopic articular cartilage evaluation and aimed to include areas of macroscopic lesions and to maximize the amount of joint surface for evaluation.

In the three elbows used for histologic evaluation of the anconeal process the aims were to: 1) obtain representative frontal plane histologic sections through the typical location of spurs of the lateral margin of the process (anconeal spur), and 2) obtain histologic sections that had a similar orientation to that used to measure the anconeal spur in CT images. The samples were taken guided by the macroscopic and CT image appearance of the anconeal process.

Samples were processed routinely for histology, embedded in paraffin wax, cut into approximately 4 μm thick sections and stained with hematoxylin and eosin. Sections from the 29 joints used for cartilage grading were additionally stained with toluidine blue, used as a complement to hematoxylin and eosin stained sections to highlight cartilage changes. Sections used for figures were photographed using a Nikon E600 light microscope and a Nikon DXM 1200 camera (Nikon Instruments, Melville, NY, USA). Light and colour adjustments were done in Adobe Photoshop version 21.1.3.

2.6. Histologic assessment of articular cartilage

Histologic changes in the cartilage were assessed and graded in coded sections by two of the authors (AL, CL) following a modification of the Osteoarthritis Research Society International (OARSI) histopathology grading system for human OA (Pritzker et al., 2006) (Suppl. Table S1). If there was disagreement between grade values, the final grade was decided by consensus. The articular cartilage of each of the five samples sites (i.e. the humeral trochlea, the humeral capitulum, the proximal half of the ulna trochlear notch, the distal half of the ulnar trochlear notch and the radius) were individually assessed for surface integrity, matrix loss, cellular change (chondrocyte hypertrophy, clustering, necrosis and loss) and depth of lesions (fibrillation, fissures, erosion, ulceration). A global cartilage score (GCS) was assigned to each joint by adding the scores for the five evaluated joint surface regions,

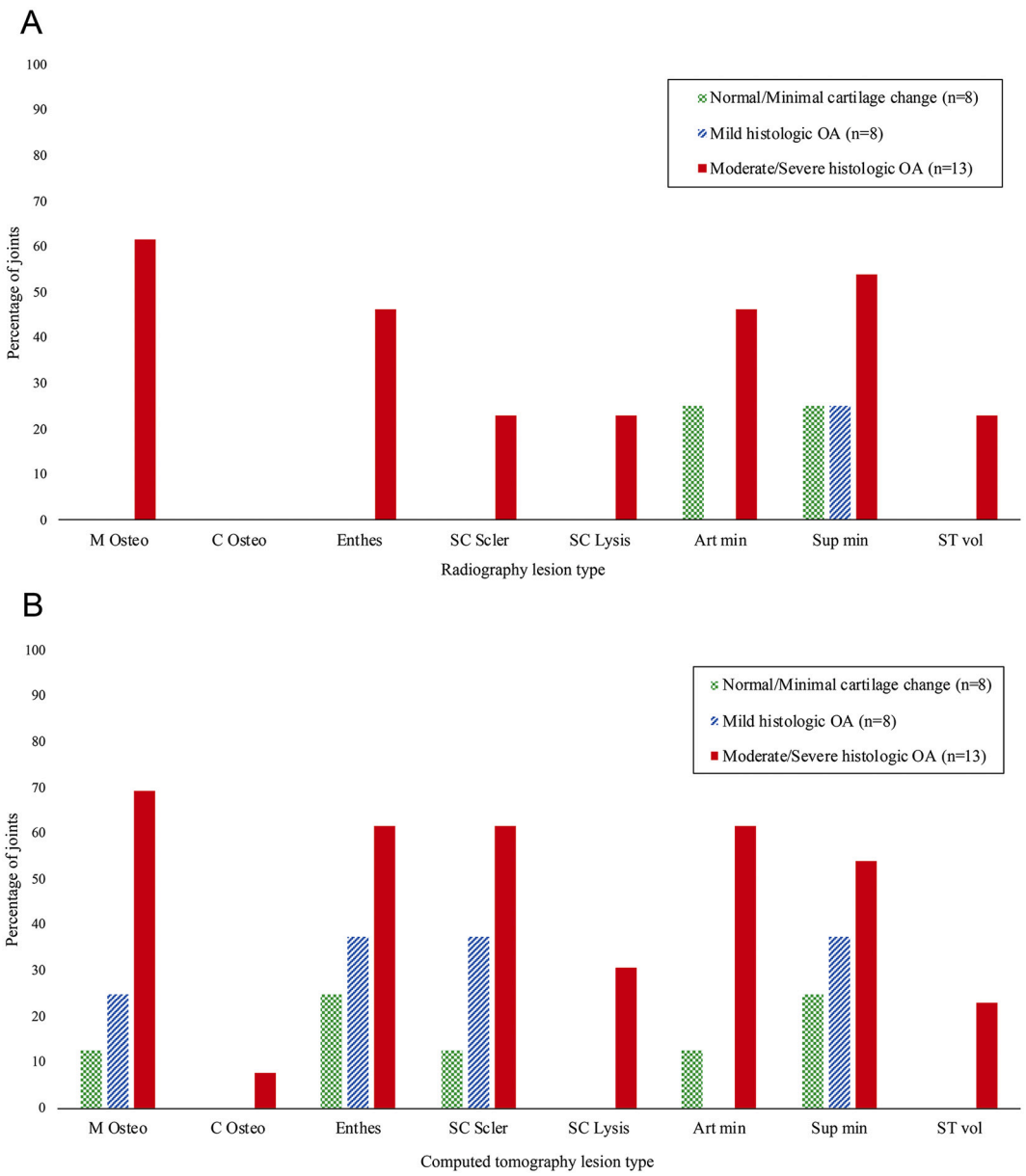

Fig. 6. Detection of lesions in radiographs (A) and computed tomography images (B) according to histologic severity in feline elbow joints (n = 29). M Osteo = marginal osteophyte, C Osteo = central osteophyte, Enthes = enthesophyte, SC Scler = subchondral bone sclerosis, SC Lysis = subchondral bone lysis (including cyst-like lesions), Art min = discrete mineral attenuation/opacity not considered to be a mineralised supinator sesamoid, Sup min = discrete mineral attenuation/opacity in the expected location of the supinator sesamoid, ST vol = increased joint soft tissue volume.

creating a maximum total score of 32.5 points. Each joint was designated a histologic severity classification based on a previous published study (Leijon et al., 2017). Due to the uncertain significance of very mild cartilage lesions in regard to the definite presence of OA, joints with GCS $\leq$ 7.5 and worst lesion 1.5–2.5 were classified as minimal cartilage change and not OA (Table 3).

2.7. Histologic appearance of CT detected anconeal spurs

One evaluator (CJL) measured the size of the anconeal spurs in elbow CT images from a separate cohort of cats examined in another study where formalin fixed elbow tissues were available. Three elbows were selected that included one anconeal spur smaller than subjective threshold for anconeal spur size for detecting elbow OA that was calculated in the results, and two anconeal spurs larger than this threshold. Once histologic sections were available the CT images were manually oriented using 3D MPR to correlate with the plane and position of the histologic section and histologic changes in the area of the anconeal spurs described.

2.8. Statistics

Associations between the predictor histologic GCS and the responses: Rad OA, CT OA, Macro OA, and anconeal spur size in CT images (mean values of three evaluators) were investigated. The binary outcomes Rad OA, CT OA and Macro OA were modeled using logistic regression (PROC LOGISTIC procedure, SAS, version 9.4, SAS Institute, Cary, NC). The continuous outcome, anconeal spur size was modeled using linear regression (PROC REG procedure, SAS, version 9.4, SAS Institute, Cary, NC) and based on these results a subjective threshold for anconeal spur size for detecting elbow OA (CT-anconeal OA) was derived. For all statistical tests' P values of $\leq$ 0.05 were considered significant.

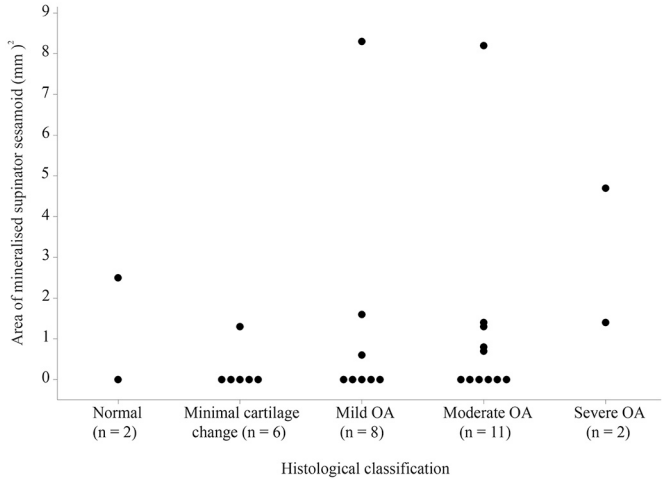

Fig. 7. Distribution of the area (mm^2) of mineralised supinator sesamoids measured in computed tomography images according to the histologic osteoarthritis (OA) classification of the joint (n = 29).

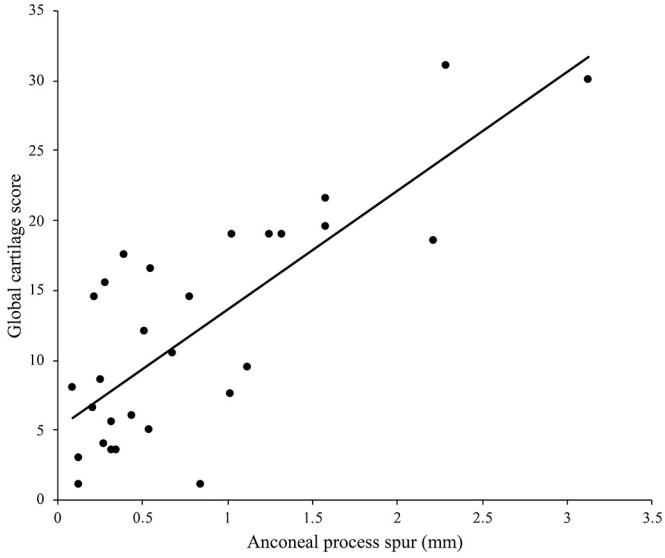

Fig. 8. Distribution of measurements of anconeal process lateral margin spurs (mean value of three readers) showing the correlation to histologic global cartilage scores in feline elbow joints (n = 29). The black line indicates the linear regression trendline.

To investigate the reliability of anconeal spur measurements the intra-class correlation (ICC) between evaluators was calculated using a custom-written macro based on a mixed procedure in SAS (SAS, version 9.4, SAS Institute, Cary, NC). ICC values were considered to indicate reliability as poor when less than 0.5, moderate between 0.5 and 0.75, good between 0.75 and 0.9 and excellent when greater than 0.9 (Koo and Li, 2016).

Using online statistical software (https://statpages.info/ctab2x2.html) the sensitivities and specificities, including 95% confidence intervals, were calculated for Rad OA, CT OA, Macro OA and CT-anconeal OA using histology as the reference standard. The histologic classifications normal and minimal cartilage change were considered OA negative. Two thresholds were used for histologic OA positive: 1) mild OA, 2) combined moderate and severe OA (Table 3). Sensitivity and specificity values <0.5 were classified as low, 0.5–0.69 as moderate, 0.7–0.89 as high and 0.9–1 as very high.

3. Results

3.1. Demographic data

The mean age (n = 29 cats) was 9.8 years (median 9, range 1–23). Sixteen cats (55.2%) were neutered males, 10 cats (34.5%) were neutered females and the remaining 3 cats (10.3%) were intact females. Twenty cats (69.0%) were Domestic Shorthair cats and 9 cats (31.0%) were pure-bred (two Persian cats, and one individual each of Norwegian Forest Cat, British Shorthair, British Longhair, Birman, Burmese, Cornish Rex and European Shorthair). Cats sampled to investigate anconeal spurs were a 5-year-old neutered female Domestic Shorthair, a 12-year-old male Domestic Shorthair, and a 14-year-old neutered male Domestic Longhair.

3.2. Histologic cartilage lesions

The GCS ranged from 1.5 to 31 (median 10.5, interquartile range (IQR) 5.25–18.75). Two joints (7%) were normal, 6 joints (21%) showed minimal cartilage changes, 8 joints (28%) mild OA, 11 joints (38%) moderate OA, and 2 joints (7%) severe OA.

Grouped by sample region the order from highest to lowest summed grades from all 29 joints were: distal ulna (summed grade 90, median grade 2.5, IQR 1.75–5), proximal ulna (summed grade 86, median grade 2.5, IQR 1.25–5), humeral trochlea (summed grade 62, median grade 1, IQR 0–4), radius (summed grade 59.5, median grade 1.5, IQR 0.5–3) and humeral capitulum (summed grade 53.5, median grade 1, IQR 0–3).

3.3. Macroscopic cartilage lesions

Macroscopic changes were minimal in 4 joints, mild in 5 joints, moderate in 5 joints and severe in 3 joints. Examples of macroscopic cartilage lesion grades are shown in Fig. 2. The distribution of macroscopic cartilage lesion grades according to the GCS is shown in Fig. 3. In 13/29 (49%) joints macroscopic cartilage lesions considered to indicate OA were detected. There was an association between the presence of Macro OA and the GCS (P = 0.0028).

3.4. Diagnostic imaging findings

There was an association between CT OA and the GCS (P = 0.0075), however there was no association between Rad OA and the GCS (P = 0.0799). Examples of diagnostic imaging lesion grades are shown in Figs. 4 and 5.

The frequency and grades of lesion types and supinator sesamoid mineralisation in radiographs and CT images according to the histologic classification are shown in Fig. 6 and Suppl. Tables S2 and S3. The distribution and size of mineralised supinator sesamoids according to the histologic classification is shown in Fig. 7. The frequency and grades of lesion types and supinator sesamoid mineralisation in radiographs and CT images according to the radiography and CT OA diagnosis are shown in Suppl. Table S4.

Mean values from the three evaluators for the measurements of spurs detected on the lateral margin of the anconeal process in CT images ranged from 0.09 to 3.13 mm (median value of 0.54 mm, 1st quartile = 0.28 mm, 3rd quartile =1.18 mm). The reliability between the evaluators' measurements was good (ICC = 0.79). There was good correlation between the size of anconeal spurs measured in CT images and the GCS ($P < 0.0001$, $R^2 = 0.61$, Fig. 8). Sixteen joints (55%) had spurs ≥0.5 mm and only 1 of these joints did not have histologic OA (GCS > 8 or worst lesion grade ≥ 3). Thirteen joints (45%) had spurs <0.5 mm and only 6 of these had histologic OA. Thus, a spur size of ≥0.5 mm was used for the CT-anconeal OA threshold.

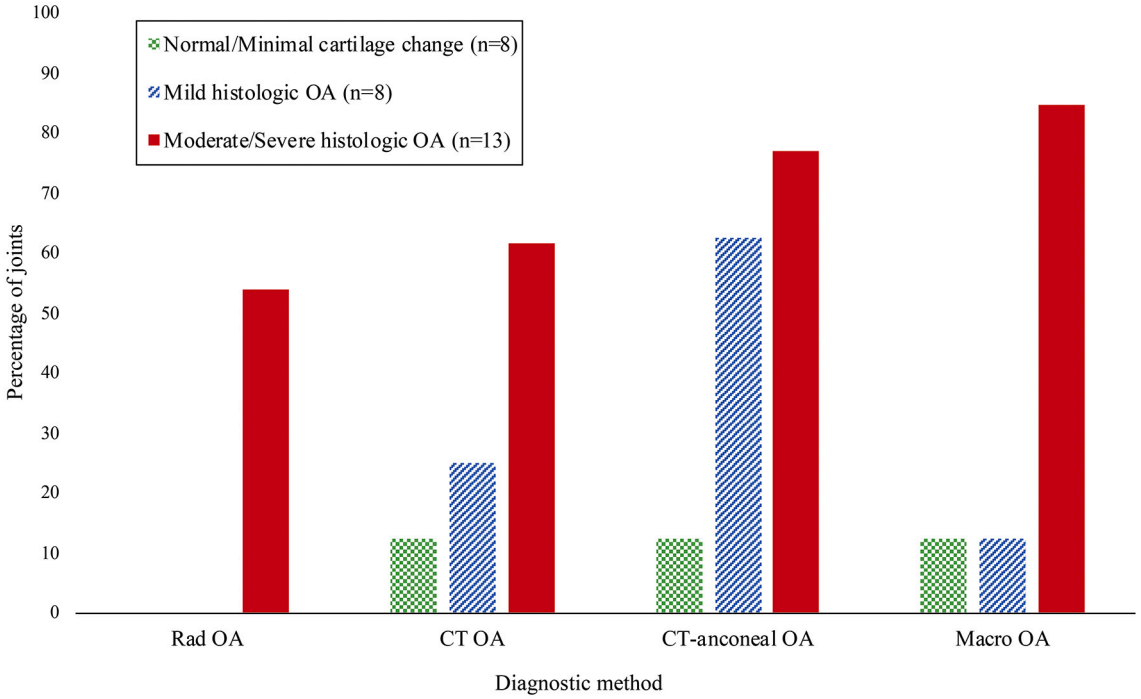

Fig. 9. Detection of feline elbow histologic osteoarthritis (OA) in 29 cats using the diagnostic techniques: radiography (Rad OA), computed tomography (CT OA), anconeal process spur measurement in computed tomography ≥0.5 mm (CT-anconeal OA), macroscopic evaluation of articular cartilage (Macro OA).

Table 4
Sensitivity and specificity for the detection of mild, and combined moderate and severe histologic osteoarthritis (OA) in feline elbow joints using diagnostic imaging methods and macroscopic examination.

	Sensitivity (95% CI)	Specificity (95% CI)
Mild histologic OA (n = 16)[a]		
Rad OA	0 (0–0.37)	1 (0.63–1)
CT OA	0.25 (0.03–0.65)	0.88 (0.47–1)
CT-anconeal OA	0.63 (0.24–0.91)	0.88 (0.47–1)
Macro OA	0.13 (0–0.53)	0.88 (0.47–1)
Moderate/severe histologic OA (n = 21)[b]		
Rad OA	0.54 (0.25–0.81)	1 (0.63–1)
CT OA	0.62 (0.32–0.86)	0.88 (0.47–1)
CT-anconeal OA	0.77 (0.46–0.95)	0.88 (0.47–1)
Macro OA	0.85 (0.55–0.98)	0.88 (0.47–1)

CT-anconeal OA = anconeal spur measurement ≥0.5 mm, CT OA = computed tomography OA-positive, Macro OA = macroscopy OA-positive, Rad OA = radiography OA-positive.

[a] includes 8 mild OA, 6 minimal cartilage lesions, 2 normal.

[b] includes 2 severe OA, 11 moderate OA, 6 minimal cartilage lesions, 2 normal.

3.5. Detection of histologic OA by radiography, CT and macroscopy

Percentages of joints with Macro OA, Rad OA, CT OA and CT-anconeal OA according to the histologic severity classification are shown in Fig. 9.

Sensitivity and specificity values for Macro OA, Rad OA, CT OA and CT-anconeal OA for the thresholds of histologic OA are shown in Table 4. For histologic OA, Rad OA had a very high specificity (1) and CT OA, CT-anconeal OA and Macro OA had a high specificity (all 0.88). For combined moderate and severe histologic OA, Macro OA and CT-anconeal OA had a high sensitivity (0.85 and 0.77 respectively), and CT OA and Rad OA had a moderate sensitivity (0.62 and 0.54 respectively). For mild histologic OA, CT-anconeal OA had a moderate sensitivity (0.63), CT OA and Macro OA had a low sensitivity (0.25 and 0.13 respectively) and Rad OA did not detect any of the joints with mild histologic OA.

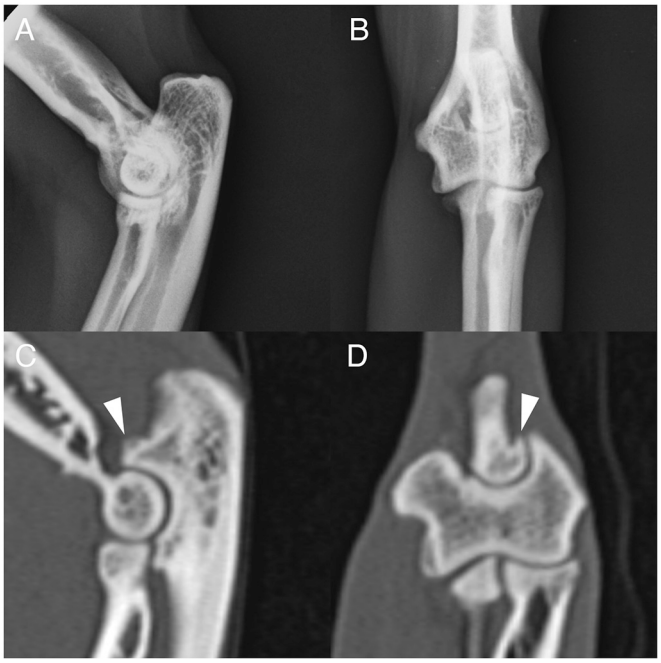

Fig. 10. Radiographs (A and B) and computed tomography (CT) images (C and D) of the same elbow joint with moderate histologic OA from a 9-year-old cat in the study showing the appearance of the anconeal process region. In the mediolateral (A) and craniocaudal (B) projection radiographs the anconeal process is summated on the humerus resulting in poor definition of the anconeal process. In the sagittal (C) and frontal (D) plane CT images a 1.58 mm size osteophytic spur (arrowheads) is seen on the lateral margin of the anconeal process.

Representative radiographs and CT images, from a joint with moderate histologic OA, graded OA positive from CT images with a large CT-

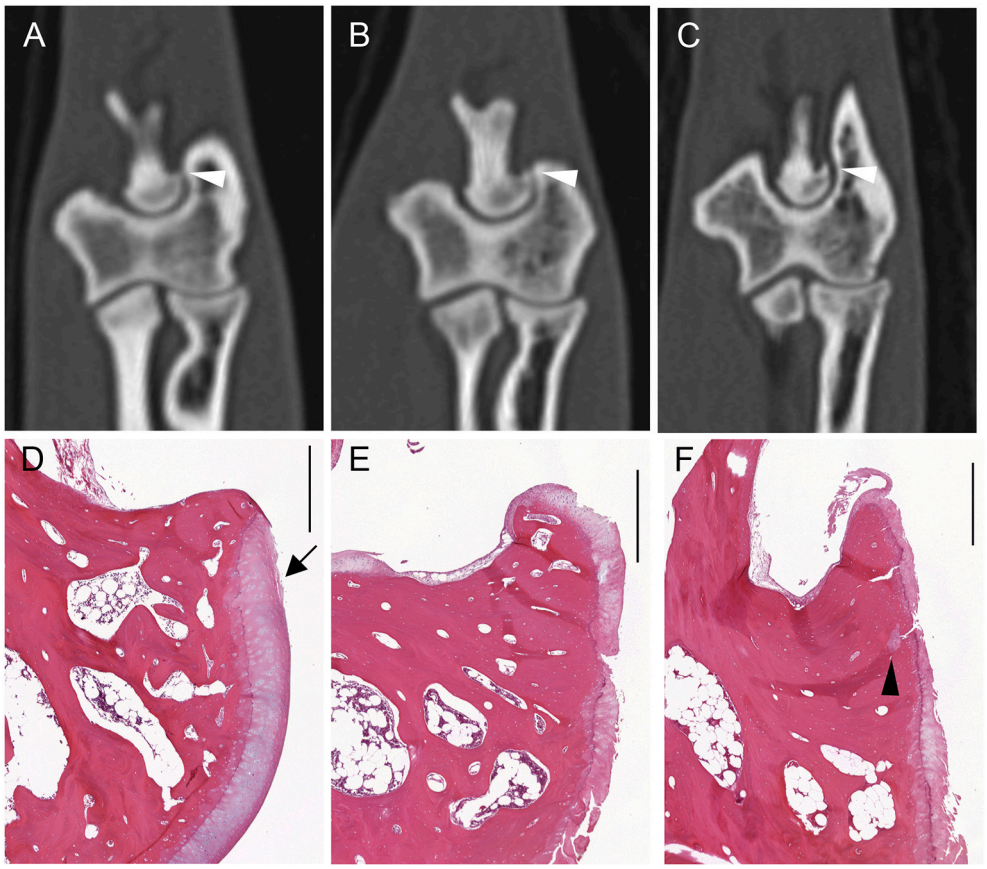

Fig. 11. Frontal plane computed tomography (CT) images (A, B, C) with corresponding histologic sections (D, E, F) of the lateral region of the anconeal process (white arrowhead), left elbow joints. (A, D) No spur formation (CT measurement 0.33 mm) on the anconeal process and mild superficial fibrillation (black arrow) of the articular cartilage in a 12-year-old cat. (B, E) Mild spur formation (CT measurement 0.82 mm) in a 5-year-old cat showing articular cartilage hypocellularity, cracks and extracellular matrix loss. (C, F) Moderate spur formation (CT measurement 1.29 mm) in a 14-year-old cat showing articular cartilage hypocellularity, cracks and extracellular matrix loss, subchondral cracks and a small focal area of chondroid tissue (black arrowhead). Histology sections are stained with hematoxylin and eosin and scale bars are 500 um.

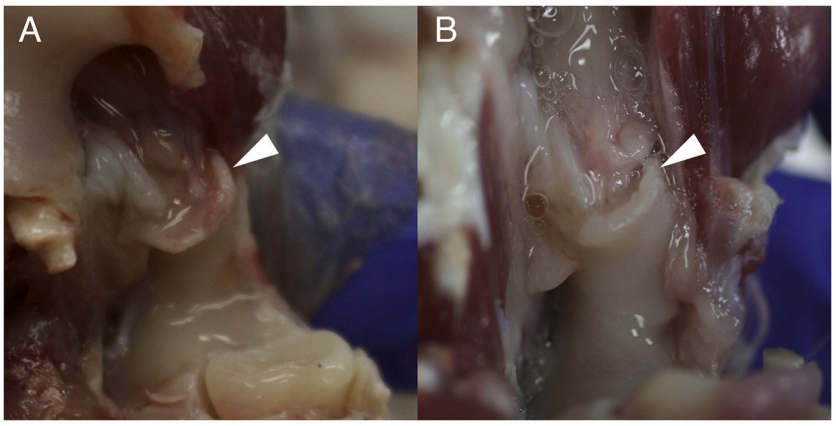

Fig. 12. Photographs of osteophytic spur formation (arrowheads) on the lateral margins of the anconeal processes of two joints shown in Fig. 11. (A) Left elbow from a 5-year-old cat shown in Fig. 11B and E, with anconeal spur measuring 0.82 mm in computed tomography images. (B) Left elbow from a 14-year-old cat shown in Fig. 11C and F, with anconeal spur measuring 1.29 mm in computed tomography images.

detected anconeal spur but that was graded OA negative from radiographs is shown in Fig. 10.

3.6. Histologic appearance of the lateral margin of the anconeal process

The three additionally sampled left elbows had 0.33 mm, 0.82 mm, and 1.29 mm anconeal spur measurements in CT images, respectively. The 0.33 mm spur (Fig. 11A and D) histologically comprised mild proximolateral bulging of mature bone Articular cartilage covered the lateral aspect of the anconeal process. Adjacent to the bulging bone the hyaline cartilage showed mild superficial fibrillation. Both the 0.82 mm and the 1.29 mm spurs showed fibrocartilage capped bone, consistent with osteophytes. The 0.82 mm spur (Fig. 11B, E and 12A) was round, whereas the 1.29 mm spur (Fig. 11C, F and 12B) was pointed and peak-shaped. The articular cartilage bordering the spurs showed severe degenerative lesions including hypocellularity, cracks and extracellular matrix loss involving the superficial, mid and deep zones of the cartilage (Fig. 11E and F). In addition, the bone of the 1.29 mm spur was sclerotic, and showed multiple subchondral cracks and focal subchondral chondroid tissue (Fig. 11F).

4. Discussion

The results of this study provide novel information about the

associations between radiological and histologic changes in feline elbow OA. Lesions detected by subjective grading of radiographs and CT images of the cat elbow joint had moderate sensitivity and high specificity for detecting moderate and severe histologic OA. The sensitivity of subjective grading of CT for mild histologic OA was low and radiography did not detect any joints with mild histologic OA. This suggests very limited use for subjective grading alone for detecting the mild stages of OA. However, measurement of spurs on the lateral margin of the anconeal process in CT images and use of a threshold of ≥0.5 mm for these measurements, resulted in high sensitivity and specificity for combined moderate and severe histologic OA and moderate sensitivity and high specificity for mild histologic OA. These findings support the study hypothesis that CT is superior to radiography for the diagnosis of feline elbow OA but only when the objective anconeal spur measurement method is used.

The high sensitivity and specificity for macroscopic articular cartilage evaluation for the detection of moderate and severe histologic OA and general increase in macroscopic cartilage grade with increasing GCS was expected. Macroscopic cartilage evaluation did however fail to detect most joints with mild histologic OA. These findings concur with previous results of a macroscopic and histologic study of feline elbow OA (Freire et al., 2014), and most likely relate to histology detecting lesions with minimal interruption of the integrity of the articular cartilage surface.

This study provides the first imaging and histologic descriptions of an osteophytic spur on the lateral margin of the anconeal process in CT images of feline elbow joints. The measurement of anconeal spurs in CT images provides a reliable, straight forward, non-invasive and objective method for detecting feline elbow OA. The study shows that the anconeal spur size increases as the articular cartilage lesions grades increase, and the results suggest that elbow joints with a spur size ≥0.5 mm are likely to have OA. Further studies on larger study populations may help to investigate if a spur size of ≥0.5 mm is the optimal threshold for detection of OA. Histology showed that the lateral aspect of the feline anconeal process is covered by articular cartilage, and this is similar to dogs (Hornof et al., 2000). This results in a distinct joint margin on the lateral aspect. Osteophytes that arise at the junction between articular cartilage and bone (marginal osteophytes) can form early in the development of OA (van der Kraan and van den Berg, 2007) and macroscopically detected osteophyte formation on the anconeal process of cats with moderate OA has been reported (Bennett et al., 2012). In dogs, the presence of osteophyte formation on the anconeal process is reported to be one of the earliest and most common radiological changes of elbow OA (Grondalen and Grondalen, 1981; Kunst et al., 2014; Olsson, 1983) and is used in screening programmes (Lappalainen et al., 2009). However, there are also reports that bone formation/convex contour on the anconeal process is not always associated with OA (Lappalainen et al., 2009) and in some cases may represent an anatomical variant or entheseopathy of the joint capsule and/or the olecranon ligament (Kunst et al., 2014). The anatomy of the olecranon ligament in cats has been described in detail (Engelke et al., 2005), and the location of the spur on the lateral margin of the anconeal process described in the current study does not correspond to the attachment of the olecranon ligament. Furthermore, both macroscopic evaluation and histologic findings in the region of the spur in the three additional joints that were collected in this study show that this region is neither an attachment for the olecranon ligament nor the joint capsule, but that the spur shaped enlargement/extension of this joint margin correspond to marginal osteophyte formation.

In dogs the proximal margin of the anconeal process can be projected without summation of the humerus in a flexed mediolateral projection radiograph (Olsson, 1983). The feline anconeal process is shorter and more blunted in shape compared to dogs. This means that even in a flexed position it is very difficult, if not impossible, to show the anconeal process in a radiograph without summation of the distal humerus. Furthermore, the spur formation observed in the CT images in the present study was on the lateral articular margin of the anconeal process, so even with a mediolateral radiographic projection that avoids summation of the distal humerus there will be summation with the anconeal process itself. This means that a small (approximately 0.5–1.5 mm) osteophytic spur is unlikely to be visible in the radiograph. This summation may be the reason that previous radiological studies of feline OA have not reported the anconeal process to be a common location for osteophyte formation. The anconeal spur was easily identified in the CT images and could be reliably measured using the CT protocol described in the current study.

The frequency of histologic OA (21/29 joints) detected in the cat elbows in this study was high and this agrees with the high frequency of feline elbow OA reported in the literature (Freire et al., 2014; Freire et al., 2011). Analysis of the distribution of grades given in the histologic samples showed that grades were highest and most frequent for the articular surfaces of the ulna followed by the humeral trochlea. This is in agreement with previous studies that have found the highest frequency of OA changes on the articular surfaces of the ulna (medial coronoid process) and the humeral condyle trochlea (Bennett et al., 2012; Freire et al., 2014) but also adds the articular surfaces of the proximal ulnar trochlear notch and anconeal process as a common location for cartilage lesions. Additionally, the finding that osteophyte formation on the lateral aspect of the anconeal process had a high sensitivity and high specificity for mild, moderate and severe histologic OA highlights the importance of evaluating this region in studies of the development and progression of OA. In the current and a previous study (Freire et al., 2014) the standard sampling method for the articular surfaces of the proximal ulna utilizes a parasagittal section through the anconeal process, trochlear notch and coronoid process. This results in histologic sections that are unlikely to allow evaluation of the lateral articular margin of the anconeal process for osteophyte formation. Inclusion of frontal plane samples that contain the lateral margin of the anconeal process in the standard joint sampling protocol for histology, and assessment for osteophyte formation and cartilage degeneration in this region are likely to be valuable for detection of elbow OA in future studies in cats.

In the current study the frequency of subchondral bone sclerosis was highest in joints with moderate and severe histologic OA and considerably higher in CT images than in radiographs. The higher frequency of detection of subchondral sclerosis in CT compared to radiographs is not surprising since cross-sectional images allows more detailed evaluation of bone structure without the confounding effect of summation. Although sclerosis is reported to be a key feature of radiographic elbow OA in cats (Bennett et al., 2012) it is also speculated to be a feature of more severe OA (Hardie et al., 2002), which is in agreement with the findings of the current study. The relatively low frequency of radiographic subchondral sclerosis in the current study also concurs with another study that reported the frequency of sclerosis in feline elbow OA (Freire et al., 2011).

Subchondral sclerosis was suspected in CT images from one joint with minimal histologic cartilage changes (considered to indicate no definite histologic OA) and this was the only lesion detected in the joint. The explanation for this sclerosis is uncertain, however a histomorphometric study of the feline humeral condyle reports subchondral bone changes in the absence of histologic changes in the overlying articular cartilage in joints with OA (Ryan et al., 2013). To further confuse the evaluation of sclerosis there is also age-related variation in bone density in cats (Cheon et al., 2012), which is likely to complicate the assessment of the subjective evaluation of subchondral sclerosis. Even if it is possible that suspected CT subchondral sclerosis in this joint with histologic minimal cartilage changes could represent a type of OA change, this change alone is not strong evidence for OA and additional changes, including osteophyte formation, should be present in CT images for a diagnosis of OA.

Both subchondral bone lysis and increased joint soft tissue volume were detected infrequently and only in joints with moderate or severe

histologic OA suggesting that these changes are not detectable in radiographs and CT images until OA is advanced. These findings concur with a radiographic study that included 25 feline elbows with mild to moderate OA where no elbows were detected with joint effusion or subchondral erosions-cysts (Freire et al., 2011).

Discrete articular mineral attenuations/opacities that were in most cases large occurred frequently in radiographs and CT of moderate and severe histologic OA and this agrees with reports in the feline OA literature (Bennett et al., 2012; Freire et al., 2014; Tas et al., 2013). There was mild disagreement between the detection of these mineralisations in radiographs and CT. Due to the cross-sectional and higher contrast images in CT it is expected that CT should have a higher accuracy for discrete articular mineralisation compared to radiography. This suggests a low number of false positives and negatives are likely when using radiographs for the detection of these mineralisations. Discrete articular mineral attenuation/opacity were detected in mild histologic OA joints suggesting that in some cases these might start to occur at an early stage of OA development.

Mineral attenuation/opacity in the location of the supinator sesamoid was present in 41% of the joints in this study, which is in agreement with the original anatomical description of this sesamoid where a sesamoid bone was detected in 40 of 110 tendons of origin of the supinator muscles (Wood et al., 1995). Mineral attenuation/opacity supinator sesamoids were seen in all histologic categories, although the frequency was higher in moderate and severe histologic OA. In the current study area measurements made in CT images were used to divide mineral attenuation supinator sesamoids into small and large categories using a cut off of 2.25 mm^2 to investigate a possible association between increasing size of the mineral attenuation sesamoid and OA. Four joints with large mineral attenuation sesamoids were detected and these were in 4 different histologic categories: normal, mild OA, moderate OA and severe OA. The remaining 7 mineral attenuation sesamoids were small and were detected in the minimal cartilage change, mild OA, moderate OA and severe OA categories. These findings suggest that the presence and size of a mineralised supinator sesamoid is not a reliable sign for detection of feline elbow OA.

Enthesophytes were more frequently detected in CT images compared to radiographs. Enthesophytes were moderately common in joints with moderate histologic OA and present in both joints with severe histologic OA. In joints with minimal cartilage changes and mild histologic OA enthesophytes were not detected in radiographs but were occasionally detected in CT images. The higher frequency detected in CT images highlights the advantage of cross-sectional CT images over two-dimensional radiographs for evaluating morphological details of bone. Osteoarthritis is a disease that involves the entire joint organ (Loeser et al., 2012) and the present study findings suggest an association between cartilage lesions and enthesophytes. In contrast, in a study of feline medial humeral epicondylitis, three out of six cats with enthesophytes lacked evidence of histologic articular cartilage damage (Streubel et al., 2012), which suggests that enthesophytes and articular cartilage lesions can develop separately. Future studies investigating osteophytes on the lateral margin of the anconeal process and elbow enthesophytes might elucidate further possible associations between feline medial humeral epicondylitis and OA.

In comparison to previous radiographic studies of feline elbows the frequency of radiographic OA in the current study (7/29 joints) was similar (Clarke et al., 2005; Hardie et al., 2002; Lascelles et al., 2010; Slingerland et al., 2011) or lower (Clarke and Bennett, 2006; Freire et al., 2011; Godfrey and Vaughan, 2018; Godfrey, 2005). The variability of the elbow OA frequency between studies is not unexpected since there is considerable variation in the methods of recruitment for these cohorts, the ages of cats and the radiographic criteria considered to represent elbow OA. Marginal osteophytes are considered an integral feature for a radiological diagnosis of OA (Bennett et al., 2012; Brandt, 1999; Guermazi et al., 2008; Hardie et al., 2002; Turmezei and Poole, 2011) and so were considered essential for a diagnosis of OA in the current study, compared to other studies where a diagnosis of OA was possible without osteophytes being present (Clarke and Bennett, 2006; Clarke et al., 2005; Freire et al., 2011; Godfrey and Vaughan, 2018; Godfrey, 2005; Lascelles et al., 2010).

In the current study a whole-body scan CT method was used to obtain CT images. The size of a domestic cat means that is it possible to include the entire body in a single CT acquisition using a clinical scanner and whole-body CT has great potential for use in OA diagnosis in a species where lameness is often challenging to detect and localise (Clarke et al., 2005; Godfrey, 2005; Hardie et al., 2002; Lascelles, 2010; Lascelles et al., 2007; Suter et al., 1998) and in OA research. Using a whole-body scan method results in image resolution limitations due to the image field of view including the entire body. However, with the CT protocol used in the current study sub-millimetre resolution was possible in the reconstructed images. This allowed reliable detection of small structures, such as the anconeal process spur, suggesting that this technique is promising for future whole-body radiological joint studies in cats.

Histologic evaluation of the articular cartilage was used as the gold standard for OA diagnosis in the current study. The strength of histology is that it provides detailed morphological information about the articular cartilage allowing detection of the early and mild stages of OA (Pritzker et al., 2006). However, it is possible that focal regions of articular cartilage changes may have been present in areas of the joints that were not sampled, and so histology may not be a perfect gold standard. In the current study samples were obtained and graded from five regions in each joint and those regions included the most common reported locations for OA changes in cats (Bennett et al., 2012; Freire et al., 2014). Both macroscopic articular cartilage evaluation and measurement of an anconeal spur using a $\geq$ 0.5 mm threshold classified one joint each as having OA when the histologic classification was OA negative. From the information available in the study, it is not possible to say if these joints were false positive OA from the macroscopic/anconeal spur evaluation or if they were false negative from the histologic evaluation.

The low number of cats in this study is a limitation and may have contributed to the wide sensitivity and specificity confidence intervals. Further studies of larger cohorts of cats would be helpful to verify the findings of this study and to test the threshold of the anconeal spur size $\geq$0.5 mm that we propose for the detection of elbow OA. Adding assessment of the lateral margin of the anconeal process to the histological evaluation of the feline elbow in future studies may be useful to increase the sensitivity of histology for elbow OA.

Further limitations of the study include the subjective grading of radiographs and CT images, and the availability of only two radiographic projections of the joints. Although the subjective grading relied on reader experience with the support of consensus, the reliance on reader experience means that the results of the subjective grading may have been different with other readers. Additionally, the lack reference material that describes the normal feline elbow CT anatomy, meant that in some cases there was uncertainty about the presence of lesions. For example, the normal shape of the feline anconeal process had not been previously described, which initiated the further investigation of the lateral margin anconeal process spur size. Measurements of the anconeal spur alone proved to be superior to the subjective grading and the addition of this measurement to subjective grading maybe even more accurate for the detection of feline elbow OA. It is also possible that the addition of further radiographic projections, including specific projections for lateral margin anconeal process spurs, may be a way to improve the sensitivity of radiographs to feline elbow OA.

5. Conclusion

Although subjective grading of radiographs and CT images was useful for detecting moderate and severe histologic OA it suffered from poor sensitivity for detecting mild histologic OA. A spur on the lateral margin of the anconeal process could be reliably measured in CT images,

and using a spur size threshold of ≥0.5 mm had a high sensitivity for moderate and severe histologic OA, a moderate sensitivity for mild histologic OA and a high specificity for all stages of OA. The histologic appearance of examples of spurs ≥0.5 mm had a typical osteophyte morphology and severe degenerative lesions were seen in the adjacent articular cartilage. To investigate if an anconeal spur size of 0.5 mm is the optimal threshold for diagnosing elbow OA further studies of larger cohorts of cats are warranted. Computed tomography examination of the feline elbow, including measurement of spur formation on the lateral margin of the anconeal process, is superior to radiography for OA diagnosis and should be considered for OA diagnosis particularly when mild OA changes are of interest.

Declaration of Competing Interest

None.

A. Leijon is currently employed by AstraZeneca AB. There are no financial interests/personal relationships which may be considered as potential competing interests.

Acknowledgements

This study was supported by the Agria and Swedish Kennel Club Research Fund (Agria och Svenska Kennelklubben Forskningsfond, grant number N2013-007). The authors sincerely thank Agneta Boström, Peder Eriksson, Albin Norman, Christina Nilsson and Vidar Skullerud, Department of Biomedical Sciences and Veterinary Public Health, Swedish University of Agricultural Sciences for skilful technical assistance and Ulf Olsson, Department of Energy and Technology, Swedish University of Agricultural Sciences for statistical assistance.

Appendix A. Supplementary data

Supplementary data to this article can be found online at https://doi.org/10.1016/j.rvsc.2021.07.025.

References

Bennett, D., Zainal Ariffin, S.M., Johnston, P., 2012. Osteoarthritis in the cat: 1. How common is it and how easy to recognise? J. Feline Med. Surg. 14, 65–75.
Brandt, K.D., 1999. Osteophytes in osteoarthritis. Clinical aspects. Osteoarthr. Cartil. 7, 334–335.
Cheon, H., Choi, W., Lee, Y., Lee, D., Kim, J., Kang, J.H., Na, K., Chang, J., Chang, D., 2012. Assessment of trabecular bone mineral density using quantitative computed tomography in normal cats. J. Vet. Med. Sci. 74, 1461–1467.
Clarke, S.P., Bennett, D., 2006. Feline osteoarthritis: a prospective study of 28 cases. J. Small Anim. Pract. 47, 439–445.
Clarke, S.P., Mellor, D., Clements, D.N., Gemmill, T., Farrell, M., Carmichael, S., Bennett, D., 2005. Prevalence of radiographic signs of degenerative joint disease in a hospital population of cats. Vet. Rec. 157, 793–799.
Engelke, E.K., Brunnberg, L., Waibl, H., 2005. Das Ligamentum olecrani des Ellbogengelenkes bei Hund und Katze. Kleintierpraxis 50, 313–323.
Freire, M., Robertson, I., Bondell, H.D., Brown, J., Hash, J., Pease, A.P., Lascelles, B.D.X., 2011. Radiographic evaluation of feline appendicular degenerative joint disease vs. macroscopic appearance of articular cartilage. Vet. Radiol. Ultrasound 52, 239–247.
Freire, M., Meuten, D., Lascelles, D., 2014. Pathology of articular cartilage and synovial membrane from elbow joints with and without degenerative joint disease in domestic cats. Vet. Pathol. 51, 968–978.
Godfrey, D., Vaughan, L., 2018. Historical prevalence of radiological appendicular osteoarthritis in cats (1972-1973). J. Am. Anim. Hosp. Assoc. 54, 209–212.
Godfrey, D.R., 2005. Osteoarthritis in cats: a retrospective radiological study. J. Small Anim. Pract. 46, 425–429.
Grondalen, J., Grondalen, T., 1981. Arthrosis in the elbow joint of young rapidly growing dogs. V. A pathoanatomical investigation. Nord. Vet. Med. 33, 1–16.
Guermazi, A., Burstein, D., Conaghan, P., Eckstein, F., Hellio Le Graverand-Gastineau, M. P., Keen, H., Roemer, F.W., 2008. Imaging in osteoarthritis. Rheum. Dis. Clin. N. Am. 34, 645–687.
Hardie, E.M., Roe, S.C., Martin, F.R., 2002. Radiographic evidence of degenerative joint disease in geriatric cats: 100 cases (1994-1997). J. Am. Vet. Med. Assoc. 220, 628–632.
Hornof, W.J., Wind, A.P., Wallack, S.T., Schulz, K.S., 2000. Canine elbow dysplasia. The early radiographic detection of fragmentation of the coronoid process. Vet. Clin. North Am. Small Anim. Pract. 30, 257–266.
Jones, G., Ding, C., Scott, F., Glisson, M., Cicuttini, F., 2004. Early radiographic osteoarthritis is associated with substantial changes in cartilage volume and tibial bone surface area in both males and females. Osteoarthr. Cartil. 12, 169–174.
Koo, T.K., Li, M.Y., 2016. A guideline of selecting and reporting Intraclass correlation coefficients for reliability research. J. Chiropr. Med. 15, 155–163.
van der Kraan, P.M., van den Berg, W.B., 2007. Osteophytes: relevance and biology. Osteoarthr. Cartil. 15, 237–244.
Kunst, C.M., Pease, A.P., Nelson, N.C., Habing, G., Ballegeer, E.A., 2014. Computed tomographic identification of dysplasia and progression of osteoarthritis in dog elbows previously assigned OFA grades 0 and 1. Vet. Radiol. Ultrasound 55, 511–520.
Lappalainen, A.K., Molsa, S., Liman, A., Laitinen-Vapaavuori, O., Snellman, M., 2009. Radiographic and computed tomography findings in Belgian shepherd dogs with mild elbow dysplasia. Vet. Radiol. Ultrasound 50, 364–369.
Lascelles, B.D., 2010. Feline degenerative joint disease. Vet. Surg. 39, 2–13.
Lascelles, B.D.X., Hansen, B.D., Roe, S., DePuy, V., Thomson, A., Pierce, C.C., Smith, E.S., Rowinski, E., 2007. Evaluation of client-specific outcome measures and activity monitoring to measure pain relief in cats with osteoarthritis. J. Vet. Intern. Med. 21, 410–416.
Lascelles, B.D.X., Henry 3rd, J.B., Brown, J., Robertson, I., Sumrell, A.T., Simpson, W., Wheeler, S., Hansen, B.D., Zamprogno, H., Freire, M., Pease, A., 2010. Cross-sectional study of the prevalence of radiographic degenerative joint disease in domesticated cats. Vet. Surg. 39, 535–544.
Leijon, A., Ley, C.J., Corin, A., Ley, C., 2017. Cartilage lesions in feline stifle joints - associations with articular mineralizations and implications for osteoarthritis. Res. Vet. Sci. 114, 186–193.
Loeser, R.F., Goldring, S.R., Scanzello, C.R., Goldring, M.B., 2012. Osteoarthritis: a disease of the joint as an organ. Arthritis Rheum. 64, 1697–1707.
Malik, R., Allan, G.S., Howlett, C.R., Thompson, D.E., James, G., McWhirter, C., Kendall, K., 1999. Osteochondrodysplasia in Scottish fold cats. Aust. Vet. J. 77, 85–92.
Olsson, S.E., 1983. The early diagnosis of fragmented coronoid process and Osteochondritis Dissecans of the canine elbow joint. J. Am. Anim. Hosp. Assoc. 19, 616–626.
Palmer, A.J., Brown, C.P., McNally, E.G., Price, A.J., Tracey, I., Jezzard, P., Carr, A.J., Glyn-Jones, S., 2013. Non-invasive imaging of cartilage in early osteoarthritis. Bone Joint J. 95-B, 738–746.
Pritzker, K.P.H., Gay, S., Jimenez, S.A., Ostergaard, K., Pelletier, J.P., Revell, P.A., Salter, D., van den Berg, W.B., 2006. Osteoarthritis cartilage histopathology: grading and staging. Osteoarthr. Cartil. 14, 13–29.
Slingerland, L.I., Hazewinkel, H.A.W., Meij, B.P., Picavet, P., Voorhout, G., 2011. Cross-sectional study of the prevalence and clinical features of osteoarthritis in 100 cats. Vet. J. 187, 304–309.
Streubel, R., Geyer, H., Montavon, P.M., 2012. Medial humeral epicondylitis in cats. Vet. Surg. 41, 795–802.
Suter, E., Herzog, W., Leonard, T.R., Nguyen, H., 1998. One-year changes in hind limb kinematics, ground reaction forces and knee stability in an experimental model of osteoarthritis. J. Biomech. 31, 511–517.
Tas, O., De Cock, H., Lemmens, P., Pool, R.R., 2013. Synovial osteochondromatosis and sclerosing osteosarcoma in a cat. Vet. Comp. Orthop. Traumatol. 26, 160–164.
Turmezei, T.D., Poole, K.E., 2011. Computed tomography of subchondral bone and osteophytes in hip osteoarthritis: the shape of things to come? Front. Endocrinol (Lausanne) 2, 97.
Voss, K., Karli, P., Montavon, P.M., Geyer, H., 2017. Association of mineralisations in the stifle joint of domestic cats with degenerative joint disease and cranial cruciate ligament pathology. J. Feline Med. Surg. 19, 27–35.
Wood, A.K., McCarthy, P.H., Martin, I.C., 1995. Anatomic and radiographic appearance of a sesamoid bone in the tendon of origin of the supinator muscle of the cat. Am. J. Vet. Res. 56, 736–738.